JOC*Article*

Is the Beckmann Rearrangement a Concerted or Stepwise Reaction? A Computational Study

Shinichi Yamabe,* Noriko Tsuchida, and Shoko Yamazaki

Department of Chemistry, Nara University of Education, Takabatake-cho, Nara 630-8528, Japan

yamabes@nara-edu.ac.jp

Received April 25, 2005

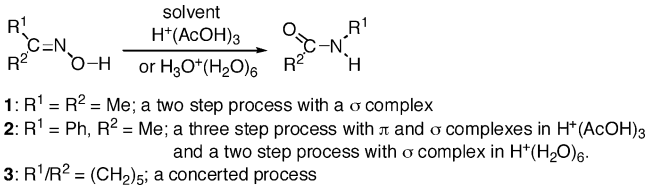

RB3LYP calculations were performed on the Beckman rearrangement by the use of three substrates, acetone oxime (**1**), acetophenone oxime (**2**), and cyclohexanone oxime (**3**). Acidic solvents were modeled by $H^+(CH_3COOH)_3$ and $H_3O^+(H_2O)_6$, and reaction paths were determined precisely. For **1**, a two-step process involving a σ-type cationic complex was obtained. For **2**, a three-step process with π- and σ-type complexes was found in $H^+(CH_3COOH)_3$ and a two-step process involving a σ-type cationic complex was obtained in $H_3O^+(H_2O)_6$. However, for **3**, a concerted process without π and σ complexes was calculated, which leads to the product, ϵ-caprolactam. Three different mechanisms were explained in terms of FMO theory.

Introduction

The Beckmann rearrangement, the conversion of an oxime into an amide,[1] was discovered in 1886 and is one of the most important methods in organic synthesis.[2] The conversion of cyclohexanone oxime into ϵ-caprolactam by this reaction is also utilized in the chemical manufacture of Nylon-6 in industry.

The Beckmann rearrangement generally requires a strong acid such as sulfuric acid or the so-called Beckmann mixture containing acetic acid, acetic anhydride, and hydrogen chloride.[2] Recently, improved methods using supercritical water,[3] vapor-phase processes,[4] and Lewis acidic ionic liquids[5] have also been reported. Several methods using catalytic activators such as *O*-alkyl-*N*,*N*-dimethylformamidium salt,[6] tetrabutylammonium perrhenate,[7] and a rhodium complex[8] have been also developed. For further improvement of the reaction conditions, now basic understanding of the precise mechanism is necessary. The general pattern of stepwise migration−fragmentation and C−O recombination reactions for the Beckmann rearrangement is outlined in Scheme 1.[2] However, the mechanism has not been elucidated explicitly. It is well-known that active participation of the surrounding solvent is crucial to control the reaction path. Nevertheless, the mechanism of the Beckmann rearrangement including solvent molecules has not yet been examined in detail.

SCHEME 1. Beckmann Reactions Adopted in This Work

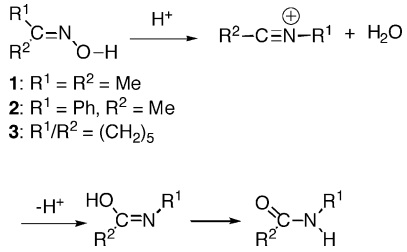

There have been various computational studies of the Beckmann rearrangement.[9] However, the adopted reaction models were not necessarily adequate. Since the

(1) Beckmann, E. *Chem. Ber*. **1886**, *89*, 988.
(2) (a) Donaruma, L. G.; Heldt, W. Z. *Org. React*. **1960**, *11*, 1. (b) Gawley, R. E. *Org. React*. **1988**, *35*, 1.
(3) (a) Ikushima, Y.; Hatakeda, K.; Sato, O.; Yokoyama, T.; Arai, M. *J. Am. Chem. Soc*. **2000**, *122*, 1908. (b) Sato, O.; Ikushima, Y.; Yokoyama, T. *J. Org. Chem*. **1998**, *63*, 9100.
(4) Izumi, Y.; Sato, Y.; Urabe, K. *Chem. Lett*. **1983**, 1649.
(5) (a) Peng, J.; Deng, Y. *Tetrahedron Lett*. **2001**, *42*, 403. (b) Ren, R. X.; Zueva, L. D.; Qu, W. *Tetrahedron Lett*. **2001**, *42*, 8441. (c) Gui, J.; Deng, Y.; Hu, Z.; Sun, Z. *Tetrahedron Lett*. **2004**, *45*, 2681. (d) Quo, K.; Deng, Y.; Yokoyama, C.; Sato, H.; Yamashita, M. *Chem. Lett*. **2004**, *33*, 1350.
(6) Izumi, Y. *Chem. Lett*. **1990**, 2171.
(7) Kusama, H.; Yamashita, Y.; Narasaka, K. *Bull. Chem. Soc. Jpn*. **1995**, *68*, 373.
(8) Arisawa, M.; Yamaguchi, M. *Org. Lett*. **2001**, *3*, 311.

10.1021/jo0508346 CCC: $30.25
Published on Web 11/23/2005

substrate oxime has nitrogen and oxygen lone-pair orbitals, hydrogen bonds from proton donors (in the acidic solution) toward the lone pairs are indispensable to describe the proton relays in the reaction. In addition, the close positions of two lone-pair orbitals and the acidic protons would bring about hydrogen-bond circuits. Computational studies reported so far were short of the environment for the substrate.

In this study, interactions between reaction substrates and solvent molecules have been precisely considered, and the reaction path and mechanism have been traced. Three substrates, acetone oxime (**1**), (*E*)-acetophenone oxime (**2**), and cyclohexanone oxime (**3**), were adopted (Scheme 1). As acidic solvents, $H^+(CH_3COOH)_3$, which is a model for "Beckmann solution" (CH_3CO_2H + HCl + $(CH_3CO_2)O$), and $H_3O^+(H_2O)_6$, which is a model for supercritical water considered as a green solvent, were used.

Calculation Methods

Density functional theory calculations were carried out by means of the hybrid functional, RB3LYP/6-31G*.[10] Geometries of reactants, transition states (TSs), and products were fully optimized. Vibrational analyses were also performed to check whether the obtained geometries are either at the energy minima or at the saddle points. From TSs, IRC calculations[11] were made to obtain the species of the energy minima (reactants, intermediates, or products). To refine energies, single-point calculations by RB3LYP/6-311+G* SCRF=PCM[12]// RB3LYP/6-31G* were performed. Relative energies shown in the geometric figures were calculated by the RB3LYP/6-311+G* SCRF=PCM electronic energies and RB3LYP/6-31G* zero-point vibrational energies. All calculations were conducted by the use of Gaussian 98[13] installed at the Information Processing Center (Nara University of Education).

Results and Discussion

Acetone Oxime (Me_2C=NOH) (1). First, two geometries of acetone oxime (**1**) were examined and are shown in Figure S1 (Supporting Information). The geometry of **1b** appears to fit better for acid coordination, because the lone-pair densities on the N2 and O3 expand in the *cis* direction. However, that of **1b** was calculated to be at a saddle point of rotation of the O3−H6 bond around the N2−O3 axis. The geometry of **1a** is at the global minimum, which is shown by the structural formula in **7A** in Figure 1.

Since the two lone-pair orbitals on N2 and O3 expand in the *trans* direction in **1a**, a hydrogen-bond circuit needs to be formed via acidic solvent molecules. Four circuit geometries are exhibited in Figure S2 (Supporting Information), where **1** and $H^+(AcOH)_3$ are involved. AcOH stands for CH_3COOH. $H^+(AcOH)_3$ is considered as a model of the Beckmann solution. Stability order of the four geometric isomers of the different H^+ positions **4A**−**7A** is **4A** > **5A** > **6A** > **7A**.[14] We attempted to find a reaction path of the rearrangement from the three complexes **4A**, **5A**, and **6A** in Figure S2. However, these were found not to lead to the reaction. The oxime O−H group in another complex **7A** (+15.8 kcal/mol relative to **4A**) is linked with two H−O groups of AcOH and $AcOH_2^+$. From the complex **7A**, i.e., precursor, a transition state **8A** (TS1) was successfully obtained and is shown in Figure 1. Scission of the N2−O3 bond and migration of the methyl group occurs at the same time. After **8A** (TS1), an intermediate **9A** composed of $(Me\text{-}C{=}N\text{-}Me)^+$ and $(AcOH)_3{\cdot}H_2O$ was calculated and is shown in Figure S3 in Supporting Information. The cation is regarded as the acetonitrile molecule coordinated by a methyl cation. The intermediate **9A** is very stable (−30.0 kcal/mol) relative to the precursor. From the intermediate **9A**, $(Me\text{-}C{=}N\text{-}Me)^+$ and $(AcOH)_3{\cdot}H_2O$, **10A** (TS2) was obtained (Figure 1), where the water molecule attacks the electrophilic carbon (C1) of the $(Me\text{-}C{=}N\text{-}Me)^+$ moiety. After **10A** (TS2), the second intermediate **11A** was produced (Figure S3), which is composed of *N*-methyl acetimidic acid (Me-C(OH)=N-Me) and $(AcOH)_3H^+$. The intermediate **11A** (ΔE = −23.5 kcal/mol) is not as stable as the first intermediate **9A** (ΔE = −30.0 kcal/mol). Isomerization of the intermediate of **11A** led to the protonated product **12A**, $(Me\text{-}COH\text{-}NH\text{-}Me)^+$ and $(AcOH)_3$, in Figure S3. This species is very stable (ΔE = −53.8 kcal/mol) owing to N-protonation. The $(Me\text{-}COH\text{-}NH\text{-}Me)^+$ moiety is the O-protonated *N*-methyl acetamide, and its deprotonation affords the product. Thus, a stepwise path consisting of **8A** (TS1), **10A** (TS2), and the two intermediates has been

(9) (a) Nguyen, M. T.; Raspoet, G.; Vanquickenborne, L. G. *J. Am. Chem. Soc*. **1997**, *119*, 2552. (b) Nguyen, M. T.; Raspoet, G.; Vanquickenborne, L. G. *J. Chem. Soc. Perkin Trans. 2* **1997**, 821. (c) Nguyen, M. T.; Raspoet, G.; Vanquickenborne, L. G. *J. Chem. Soc., Perkin Trans. 2* **1995**, 1791. (d) Nguyen, M. T. *Int. J. Mass Spectrom. Ion Proc*. **1994**, *136*, 45. (e) Nguyen, M. T.; Vanquickenborne, L. G. *J. Chem. Soc., Perkin Trans. 2* **1993**, 1969. (f) Otto, A. H. *J. Mol. Struct. (THEOCHEM)* **1991**, *81*, 489. (g) Hunt, P. A.; Pzepa, H. S. *J. Chem. Soc., Chem. Commun*. **1989**, 623. (h) Fois, G. A.; Ricchiardi, G.; Bordiga, S.; Busco, C.; Dalloro, L.; Spanò, G.; Zecchina, A. In *Proceedings of the 13th International Zeolite Conference*; Elsevier Science: New York, 2001; p 149. (i) Yamaguchi, Y.; Yasutake, N.; Nagaoka, M. *J. Mol. Struct. (THEOCHEM)* **2003**, *639*, 137. (j) Boero, M.; Ikeshoji, T.; Liew, Ch. Ch.; Terakura, K.; Parrinello, M. *J. Am. Chem. Soc*. **2004**, *126*, 6280. (k) Bucko, T.; Hafner, J.; Benko, L. *J. Phys. Chem. A* **2004**, *108*, 11388.

(10) (a) Becke, A. D. *J. Chem. Phys*. **1993**, *98*, 5648. (b) Lee, C.; Yang, W.; Parr, R. G. *Phys. Rev. B* **1998**, *37*, 785.

(11) (a) Fukui, K. *J. Phys. Chem*. **1970**, *74*, 4161. (b) Gonzalez, C.; Schlegel, H. B. *J. Phys. Chem*. **1987**, *90*, 2154.

(12) (a) Miertus, S.; Scrocco, E.; Tomasi, J. *Chem. Phys*. **1981**, *55*, 117. (b) Miertus, S.; Tomasi, J. *Chem. Phys*. **1982**, *65*, 239.

(13) Frisch, M. J.; Trucks, G. W.; Schlegel, H. B.; Scuseria, G. E.; Robb, M. A.; Cheeseman, J. R.; Zakrzewski, V. G.; Montgomery, J. A., Jr.; Stratmann, R. E.; Burant, J. C.; Dapprich, S.; Millam, J. M.; Daniels, A. D.; Kudin, K. N.; Strain, M. C.; Farkas, O.; Tomasi, J.; Barone, V.; Cossi, M.; Cammi, R.; Mennucci, B.; Pomelli, C.; Adamo, C.; Clifford, S.; Ochterski, J.; Petersson, G. A.; Ayala, P. Y.; Cui, Q.; Morokuma, K.; Malick, D. K.; Rabuck, A. D.; Raghavachari, K.; Foresman, J. B.; Cioslowski, J.; Ortiz, J. V.; Stefanov, B. B.; Liu, G.; Liashenko, A.; Piskorz, P.; Komaromi, I.; Gomperts, R.; Martin, R. L.; Fox, D. J.; Keith, T.; Al-Laham, M. A.; Peng, C. Y.; Nanayakkara, A.; Gonzalez, C.; Challacombe, M.; Gill, P. M. W.; Johnson, B. G.; Chen, W.; Wong, M. W.; Andres, J. L.; Head-Gordon, M.; Replogle, E. S.; Pople, J. A. *Gaussian 98*, revision A.11.1; Gaussian, Inc.: Pittsburgh, PA, 1998.

(14) The reactant **7A** is less stable than its isomer **4A**, **5A**, and **6A** in Figure S2. The isomer **4A** is very stable, because it contains the N-protonated moiety. Since the proton affinity (PA) of ammonia, PA-(NH_3) = 204 kcal/mol, is much larger than that of water, $PA(H_2O)$ = 165 kcal/mol (Hunter, E. P.; Lias, S. G. *J. Phys. Chem. Ref. Data* **1998**, *27*, 413), the species with the N-protonated form is generally stabilized. On the other hand, the N-protonated species are not directly related to Beckmann rearrangement. The instability of the reactant **7A** arises from absence of the N···H−O hydrogen bond. The fourth AcOH molecule would be bound to the reactant by a catalytic role. To check the role, geometries of Me_2C=NH and $H^+(AcOH)_4$ have been optimized by addition of AcOH to the geometries of $Me_2C{=}NOH(AcOH)_3H^+$ of **4A**, **5A**, **6A**, and **7A** as initial structures. The structures **4AA**, **5AA**, **6AA**, and **7AA** are shown in Figure S12 in Supporting Information. Comparing the energies of these four isomers, their stabilities are comparable. Thus, while the fourth AcOH molecule works as a catalyst, the three AcOHs work to convey the H_2O molecule from the N2 site to the C1 site. The catalytic role of the fourth AcOH molecule may be understandable in the TS geometry in Figure S13; it becomes distant from the reacting region. The fourth AcOH molecule gives ca. 20 kcal/mol stabilization to the reacting system.

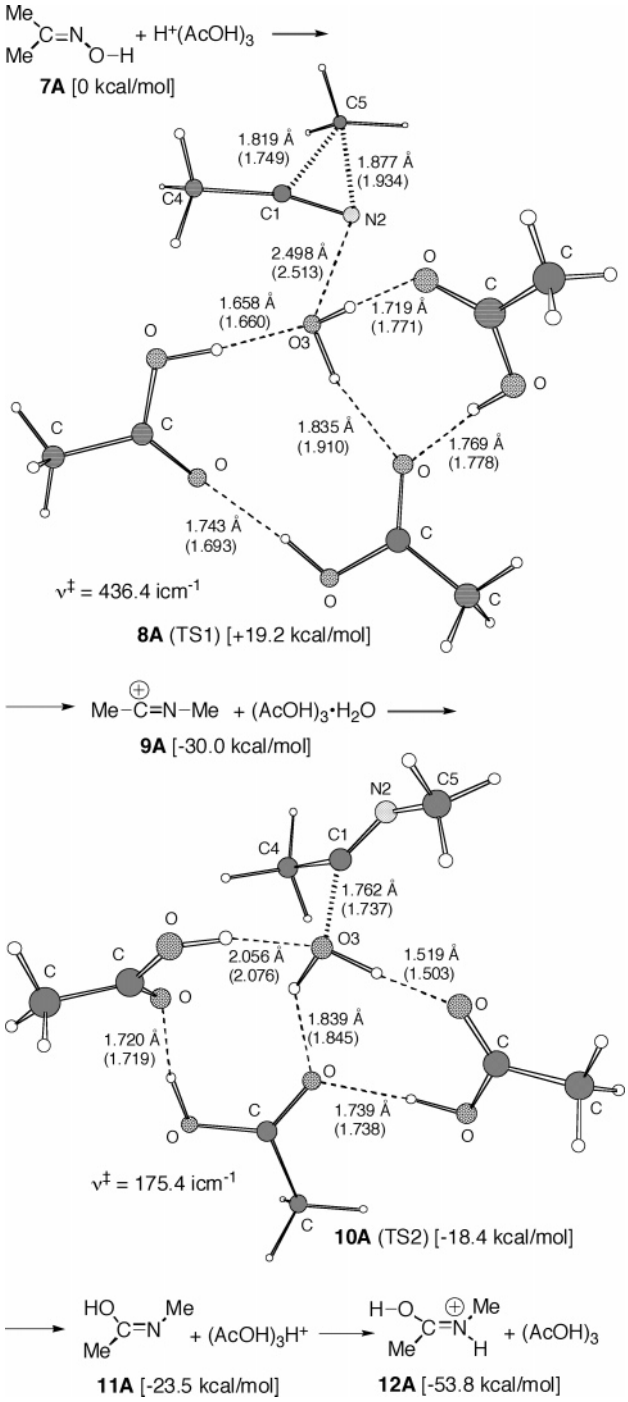

FIGURE 1. Reaction paths of the fragmentation and recombination in Scheme 1. The system is composed of $Me_2C{=}NOH$ (**1**) + $H^+(CH_3COOH)_3$. The optimized geometries of **8A** (TS1) and **10A** (TS2) are shown along with their sole imaginary frequencies, $\nu^‡$. The SCRF = dipole containing geometric data are also shown in parentheses. The geometry of **7A** is in Figure S2, and those of **9A**, **11A** and **12A** are in Figure S3 (Supporting Information). Reaction-coordinate vectors corresponding to $\nu^‡$ in **8A** (TS1) and **10A** (TS2) are also shown in Figure S3.

obtained. The AcOH trimer accepts and releases a proton flexibly toward the substrate sites via hydrogen bonds; **8A** (TS1) is the rate-determining step, and its calculated activation energy is 19.2 kcal/mol.

The most fundamental solvent, water, was adopted in a $Me_2C{=}NOH + H_3O^+ + 6H_2O$ system (Scheme 2).

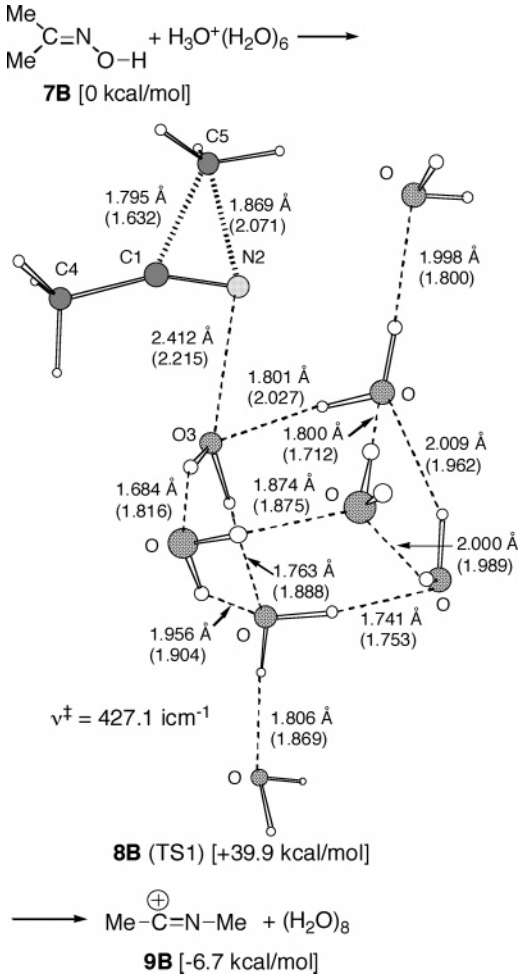

FIGURE 2. Beckmann rearrangement path up to the intermediate in the $Me_2C{=}NOH + H_3O^+ + (H_2O)_6$. The structures of **7B** and **9B** are shown in Figure S4 in Supporting Information.

SCHEME 2. Reaction Model for Beckmann Rearrangement To Examine the Catalytic Effect of One H_3O^+ and Six H_2O Molecules on Substrate 1

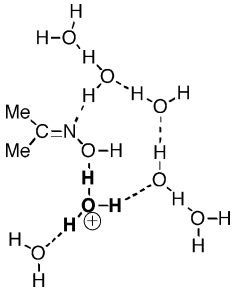

Nguyen et al.[9a] reported that they could not locate the cyclic TS shown below despite an intensive search.

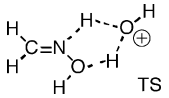

We attempted to determine the TS structure of a much larger size, $Me_2C{=}NOH + H_3O^+ + 6H_2O$, compared to the unobtainable TS structure, $H_2C{=}NOH + H_3O^+ + H_2O$. Figure 2 shows the reaction path of the first step

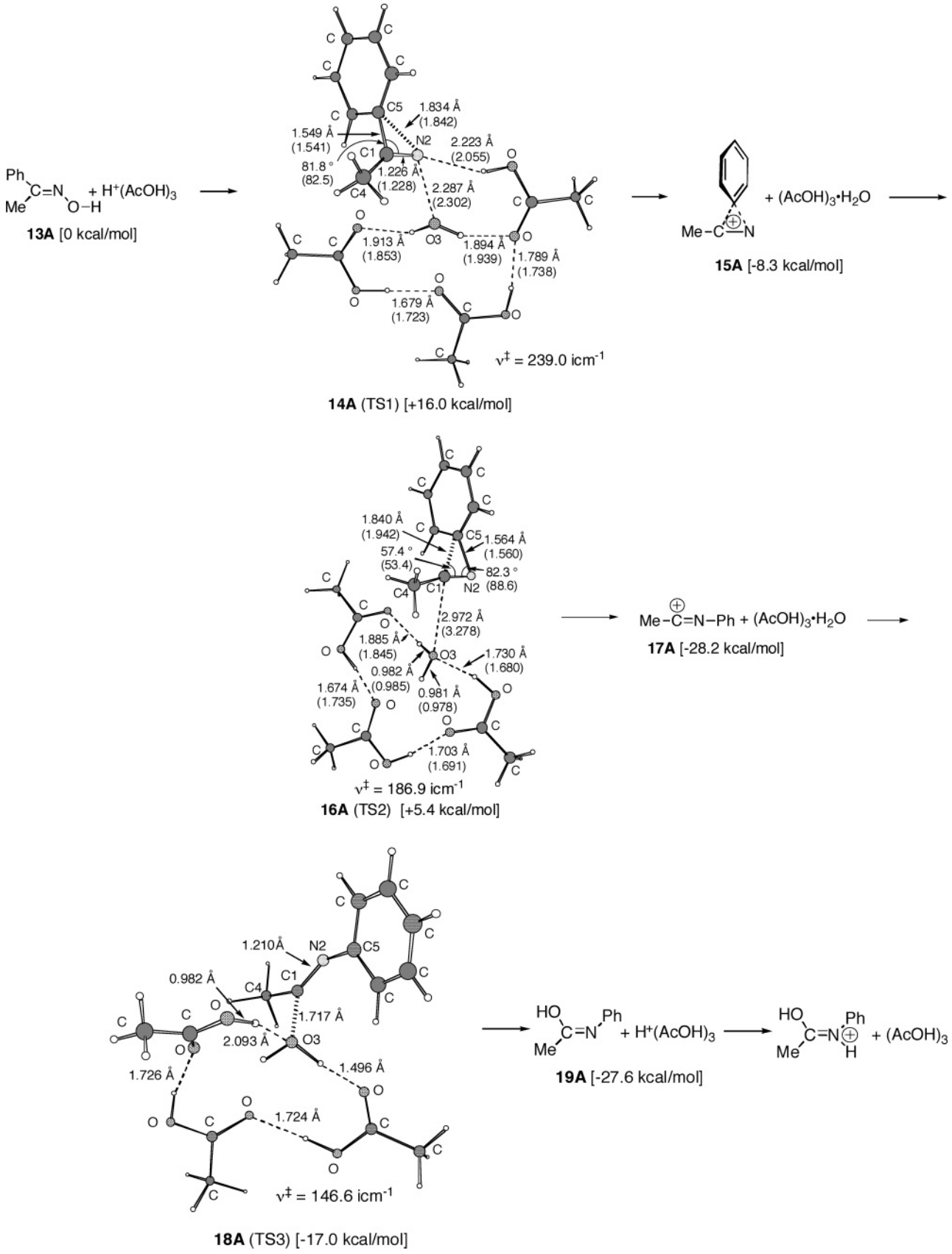

FIGURE 3. Reaction paths of the fragmentation, isomerization, and recombination. The system is composed of (*E*)-MePhC=NOH + $H^+(CH_3COOH)_3$. Geometries of **13A**, **15A**, **17A**, and **19A** are in Figure S5 in Supporting Information.

(up to the Me-C=N-Me^+ intermediate).[15] The geometry of the (Me-C=N···Me···H_2O) moiety in **8B** (TS1) is similar to that of Figure 1. That is, the rearrangement pattern is similar in the Beckmann and "aqueous" solvents, but

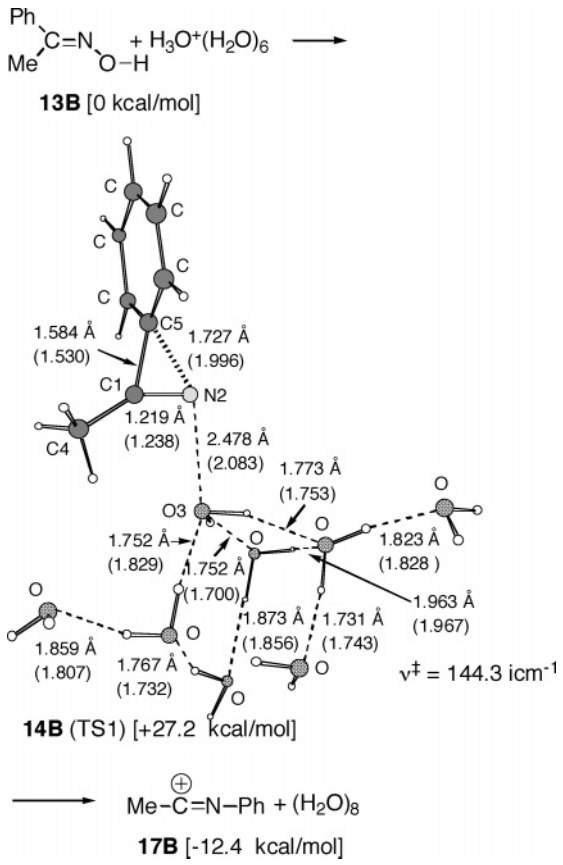

FIGURE 4. Beckmann phenyl rearrangement path up to the intermediate in the (*E*)-MePhC=NOH + H_3O^+ + $(H_2O)_6$. The structures of **13B** and **17B** are shown in Figure S6 in Supporting Information.

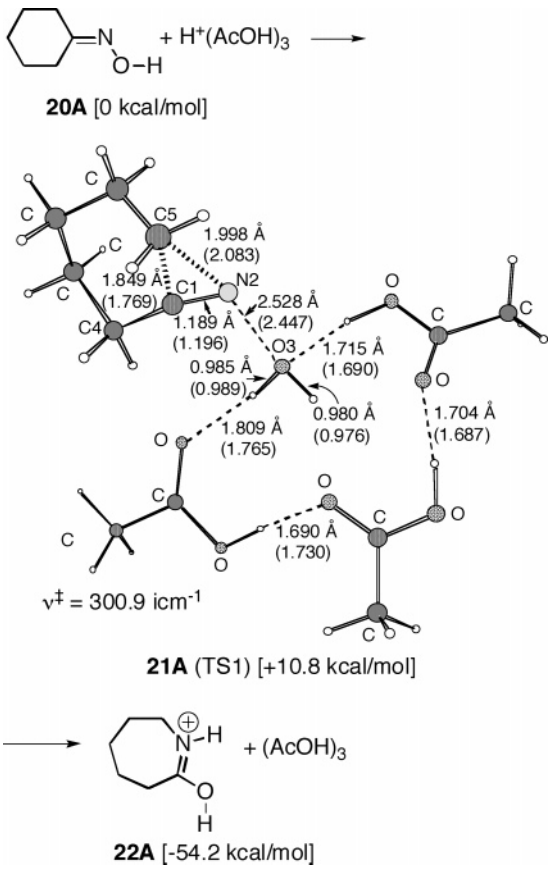

FIGURE 5. Concerted reaction path of the Beckmann rearrangement, [**3** + $H^+(CH_3COOH)_3$] → [protonated ϵ-caprolactam + $(CH_3COOH)_3$]. Geometries of **20A** and **22A** are in Figure S7 in Supporting Information.

the activation energies are crucially different between E_a (TS1) = 19.2 kcal/mol in Figure 1 and E_a (TS1) = 39.9 kcal/mol in Figure 2. The $H^+(AcOH)_3$ solvent in **7A** works more effectively to elongate the N2−O3 bond for scission than the $H_3O^+(H_2O)_6$ solvent in **7B** (1.470 Å in **7A**, 1.428 Å in **7B**). The effectiveness lowers the energy barrier arising from the N−O bond cleavage in **8A**.

In both solvents, $H^+(AcOH)_3$ and $H_3O^+(H_2O)_6$, the first step of the Beckmann rearrangement (TS1) has been shown to be a concerted process with Me migration and N−O cleavage. A (Me-C=N-Me)$^+$ intermediate is yielded, which is subject to nucleophilic attack by a H_2O molecule.

(*E*)-Acetophenone Oxime (Ph(Me)C=NOH) (2). The phenyl migration was examined here by the use of the $H^+(AcOH)_3$ solvent. The precursor geometry **13A** is shown in Figure S5 in Supporting Information, and the TS1 geometry **14A** is shown in Figure 3. Although the extent of N···O bond cleavage in **14A** (TS1) is similar to those in Figures 1 and 2, the position of the migrating group (Ph) in **14A** is entirely different from those (Me) in Figures 1 and 2. The C1−C5 bond is 1.549 Å and is not elongated at all. After **14A** (TS1), a new π complex **15A** is afforded (Figure S5). The structure of the obtained π complex was suggested before, but existence as a transition state or a transient intermediate was not exactly characterized.[2] The complex is 8.3 kcal/mol more stable than the precursor. The complex is isomerized via **16A** (TS2) to the σ complex **17A** with a energy barrier of +13.7 (= 5.4 − (−8.3)) kcal/mol. The σ complex (Me-C=N−Ph)$^+$ in **17A** is similar to (Me-C=N-Me)$^+$ shown in Figures 1 and 2. The σ complex is suitably positioned toward the evolved H_2O molecule for the subsequent nucleophilic attack. The attack is shown by **18A** (TS3). The resultant species is Me-C(OH)=N−Ph in **19A**, which is subject to the N-protonation leading to the protonated product. Thus, the phenyl migration has been found to involve π and σ complexes. Among **14A** (TS1), **16A** (TS2), and **18A** (TS3), **14A** (TS1) is the rate-determining step.

The phenyl group migration in the $H_3O^+(H_2O)_6$ solvent was examined (Figure 4). Interestingly, the π complex (phenonium ion-like) has not been obtained. The transient intermediate seems to be unstable, when a highly nucleophilic H_2O molecule in $H_3O^+(H_2O)_6$ is bound to the backside of the phenonium ion.

The *Z*−*E* isomerization for acetophenone oxime was also examined.[16] First, the *Z*−*E* isomerization path has been sought by the use of a model system, Me_2C=NOH. In the neutral system, isomerization paths were not found; the rotation about the C=N bond is not feasible. The isomerization has been investigated by the use of the reactant **13A**. The path was determined successfully

(15) Since the whole process has been shown in Figure 1 for the Me_2C=NH + $H^+(AcOH)_3$ system, only the important steps ([1,2] migration and H_2O nucleophilic attack) are shown for the other system hereafter.

(16) Johnson, J. E.; Morales, N. M.; Gorczyca, A. M.; Dolliver, D. D.; McAllister, M. A. *J. Org. Chem*. **2001**, *66*, 7979.

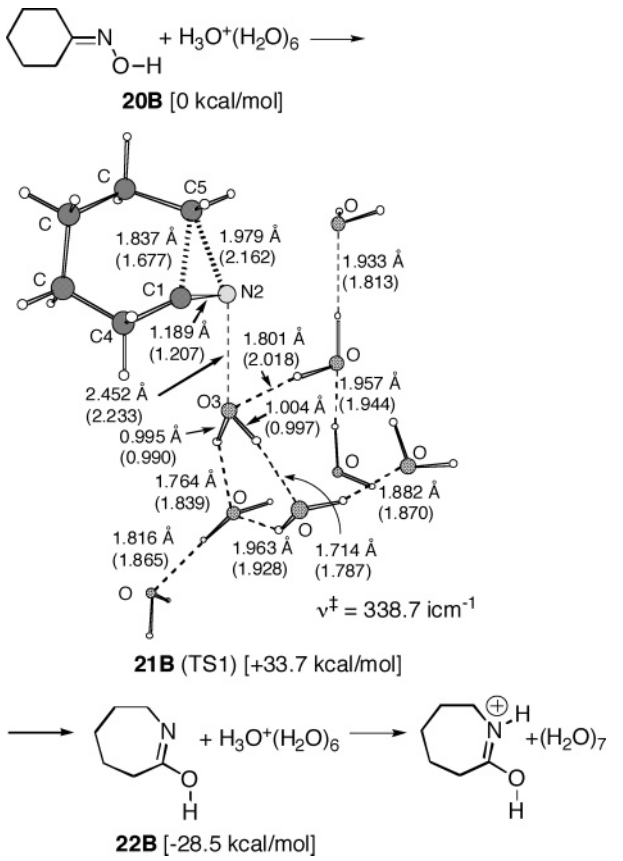

FIGURE 6. Concerted path of [**3** + H_3O^+ + $(H_2O)_6$] → [an isomer of ϵ-caprolactam + H_3O^+ + $(H_2O)_6$]. The structures of **20B** and **22B** are shown in Figure S8 in Supporting Information.

and is shown in Figure S9 in Supporting Information. The isomerization was found to occur in the N-protonated form. The activation energy is somewhat large, 39.5 kcal/mol, probably because the hydrogen-bond circuit by the AcOH trimer hinders the rotation. Thus, the isomerization may take place with *N*-protonation and without the strong solvation of outer hydrogen bonds.

Next, methyl migration for (*Z*)-acetophenone oxime was examined. Methyl migration paths in $H^+(AcOH)_3$ solvent and in $H_3O^+(H_2O)_6$ solvent are shown in Figures S10 and S11, respectively. The activation energies are E_a = 17.2 kcal/mol for $H^+(AcOH)_3$ solvent and E_a = 36.4 kcal/mol for $H_3O^+(H_2O)_6$ solvent. They are larger than those of phenyl migration in **2** (16.0 kcal/mol for $H^+(AcOH)_3$ and 31.8 kcal/mol for $H_3O^+(H_2O)_6$), respectively. The result is in good agreement with the general migratory aptitude of substituents (Ph > Me). Thus, it is likely that *Z*−*E* isomerization competes with methyl migration for (*Z*)-acetophenone oxime.

Cyclohexanone Oxime ($(CH_2)_5C$=NOH) (3). Here, the ring-strained migration was investigated. The precursor geometry composed of **3** and $H^+(AcOH)_3$ **20A** is shown in Figure S7. From the precursor **20A**, the TS1 geometry **21A** was located (Figure 5). After **21A** (TS1), the IRC-forward path leads not to the π or σ complex but to the product, the protonated ϵ-caprolactam **22A** (Figure S7) directly! The Beckmann rearrangement of **3** has been found to be a perfect concerted process, which is thoroughly different from those of acetone oxime (**1**) and

SCHEME 3. FMO Scheme[a]

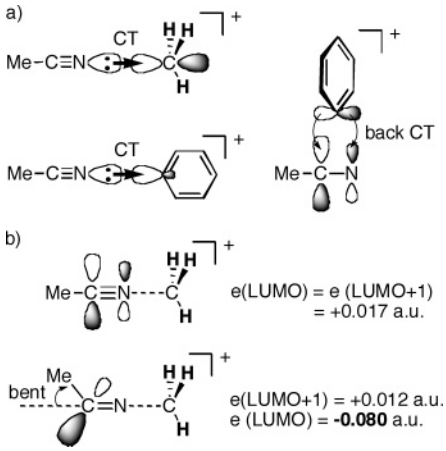

[a] (a) Charge-transfer (CT) interactions to give σ complexes, and the back CT interaction to give the π complex. (b) Changes of energies, *e*(LUMO) and *e*(LUMO+1), of the vacant frontier orbitals. When the Me-C−N axis is bent (∠Me−C−N = 130°) arbitrarily, the energy level of LUMO lowers considerably (−0.080 au).

acetophenone oxime (**2**). The activation energy (E_a = 10.8 kcal/mol) is smaller than those (19.2 kcal/mol for **1** and 16.0 kcal/mol for **2**) of the acyclic substrates. The order of the calculated E_a (**3** < **2** < **1**) is in good agreement with that of the reported experimental data E_a for Beckmann rearrangement of oxime *p*-toluenesulfonates of **1**, **2**, and **3** in acetic acid.[17]

A reacting system composed of **3** and $H_3O^+(H_2O)_6$ was examined, which is a model pertinent to the experiment using the supercritical water.[3] The reaction path in Figure 6 demonstrates again that the rearrangement is concerted and involves no intermediates. The activation energy, E_a = 33.7 kcal/mol, is smaller than that (39.9 kcal/mol) for acetone oxime (Me_2C=NOH) (**1**).

FMO Analyses of π and σ Intermediates

The Me_2C=N^+ cation is absent and is isomerized to the σ complex, Me-C=N-Me^+, during the geometry optimization. The σ and π complexes are characterized by FMO interactions in Scheme 3.

The σ complexes are generated by charge-transfer (CT) interactions from the N-σ lone pair orbital to the vacant σ orbitals of methyl and phenyl cations, respectively. They are typical coordination bonds. The π complex is afforded by the antisymmetric back CT. The extent of the back CT is much smaller than that of CT. However, the back CT may work effectively to stop the slide shift of the phenyl group.[18] The back CT also works in Cram's phenonium ion.[19] The methyl group does not have a donor antisymmetric orbital, and accordingly the π complex has not been obtained in Figures 1 and 2.

Whereas acyclic substrates **1** and **2** may have linear σ complexes, the cyclic substrate **3** cannot have the linear complex owing to ring strain. The effect of the nonlinearity on the FMO vacant orbitals was examined in Scheme 3b. In the linear σ complex, LUMO and LU-

(17) (a) Heldt, W. Z. *J. Org. Chem.* **1961**, *26*, 1695. (b) Vinnik, M. I.; Zarakhani, N. G. *Russ. Chem. Rev.* **1967**, *36*, 51.
(18) Yamabe, S.; Minato, T. *Bull. Chem. Soc. Jpn.* **1993**, *66*, 3339.
(19) Cram, D. J. *J. Am. Chem. Soc.* **1964**, *86*, 3767.

SCHEME 4. Three Mechanisms of Beckmann Rearrangement Derived from the Present Calculations

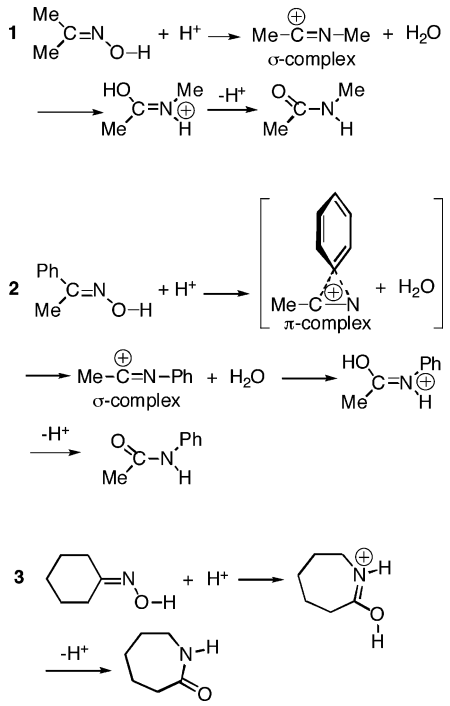

MO+1 are degenerate (same energies). When some distortion, i.e., bending, is imposed on the complex geometry, energy levels of LUMO and LUMO+1 are split. The LUMO level is lowered significantly (+0.017 → −0.080 au), which means the enhancement of the electrophilicity of the cyano carbon. Thus, the transient bent shape makes the carbon too electrophilic for the σ complex to intervene. The concerted process of the cyclohexanone oxime (**3**) has been explained in terms of the "too strong" electrophilicity toward the H_2O nucleophile to ensure the intervention.

Concluding Remarks

The Beckmann rearrangement has been investigated computationally by employment of three substrates and two solvent groups. The proton relay between the substrate and the solvent molecules controls the reaction. The migration and the N−O bond scission take place simultaneously. For the acetone oxime (**1**) and acetophenone oxime (**2**), σ complex intermediates are formed. For **2**, the π complex is also formed prior to the σ complex in the $H^+(AcOH)_3$ solvent. The evolved H_2O molecule attacks the cationic carbon of the σ complex leading to the products. The cyclohexanone oxime (**3**) undergoes the migration concertedly. Now, Scheme 1 raised in the introduction is revised to Scheme 4.

Supporting Information Available: Figures S1−S13 and the Cartesian coordinates of the optimized geometries of Figures S1−S8 and Figures 1−6. This material is available free of charge via the Internet at http://pubs.acs.org.

JO0508346